



# Magnetically Tunable Wideband Ferrite-Based Metamaterial Phase Shifter

Huiming Yao, Shihong Wang, Ming Lei and Ke Bi\*

## Abstract

Tunable phase shifters with wide bandwidth are highly demanded for phased array radar systems. However, most wideband phase shifters are not tunable, while tunable phase shifters operate at a very narrow band. Here, we present a magnetically tunable wideband ferrite-based metamaterial phase shifter by periodically arranging ferrite block and air-gap. Compared to the conventional phase shifter, the operation bandwidth of the metamaterial phase shifter increases significantly because of the existence of a new resonant peak. Meanwhile, the phase shift of the metamaterial phase shifter can be altered by changing the applied magnetic field. The proposed phase shifter has low insertion loss and large phase shift value, which provides a way to the design of tunable wideband phase shifters.

**Keywords:** Ferrite phase shifter; Wideband; Metamaterial; Magnetically tunable.

Received: 13 September 2021; Accepted: 7 October 2021.

Article type: Research article.

## 1. Introduction

Phase shifters are the key components of transmit-receive (T/R) modules and have been widely used in phased array radar systems.<sup>[1-3]</sup> Considering the importance of anti-interference and wideband imaging performance, wideband passive radars have become a research focus.<sup>[4-5]</sup> Additionally, tunable devices have also attracted great interest in recent years due to their reconfigurability.<sup>[6-8]</sup> Therefore, wide bandwidth characteristic and adjustable ability are becoming the most important design targets for phase shifters.<sup>[9-11]</sup> Owing to the negative effective permeability of ferrite materials at microwave frequencies and their dependence on the applied magnetic field, making these media the main materials to realize tunability.<sup>[12-14]</sup>

Though many studies have been carried out for tunable or wideband phase shifters, the wideband phase shifters are not tunable, while operating band of most tunable phase shifters are particularly narrow. Furthermore, most designs are complex and not easy to be integrated into the systems.<sup>[15-18]</sup> Metamaterial, due to its extraordinary electromagnetic properties, is extensively applied in various electromagnetic devices and provides many potential applications.<sup>[19-21]</sup> By applying metamaterial to the design of phase shifters can

simplify the structure of phase shifters, as well as improve their phase shift performances.<sup>[22-25]</sup> For instance, a toroidal ferrite-based metamaterial phase shifter was proposed and the miniaturization of the phase shifter was realized.<sup>[26]</sup> It is also a breakthrough that a tunable metamaterial phase shifter was presented by using composite right/left-handed (CRLH) structure.<sup>[27]</sup> In contrast to traditional phase shifters, the metamaterial phase shifters are easy to design and fabricate, which provide a new method for phase shifters design.

In this paper, a tunable wideband metamaterial phase shifter with compact size, large phase shift value and low insertion loss is presented. Size optimization is implemented to determine all parameters of the proposed phase shifter. From the simulated results, it is found that the proposed phase shifter shows a bandwidth of 1.9 GHz for a phase shift about 180°. Moreover, the phase shift value varies with the applied magnetic field. This design realizes adjustability and wideband in the meantime, and most importantly the proposed phase shifter is simple in structure. This work widens the way for the tunable wideband phase shifters design.

## 2. Phase shifter geometry and design

Phase shifters are used to adjust the phase of electromagnetic waves, which can be achieved by changing the length of signal transmission or phase constant. The permeability of ferrite materials varies with the applied magnetic field, making these media the main materials to realize magnetically tunable characteristic. In addition, ferrite phase shifters can be divided

School of Science, Beijing University of Posts and Telecommunications, Beijing 100876, China.

\*E-mail: [bike@bupt.edu.cn](mailto:bike@bupt.edu.cn) (K. Bi)

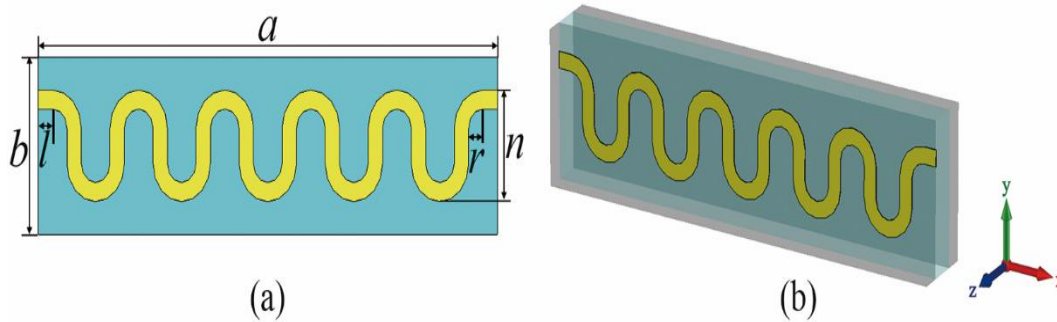


**Fig. 1** Structure of the original phase shifter (a) top view and (b) perspective view.

into waveguide type and microstrip type according to the type of transmission line. And microstrip ferrite phase shifters are widely used due to their simpler structure. In this work, a magnetically adjustable ferrite phase shifter with rectangular section is designed based on the meander line microstrip structure. The top view and perspective view of the phase shifter are respectively shown in Figs. 1a and 1b. The upper and lower layers of the structure are rectangular ferrite plates, and the middle layer is FR4 substrate with a relative dielectric constant of 2.2.

As is known to all that the performances of ferrite phase shifters are greatly affected by the materials properties and structural sizes. Saturation magnetization ( $4\pi M_s$ ) and ferromagnetic resonance linewidth ( $\Delta H$ ) are two vital parameters used to measure the electromagnetic properties of ferrite materials. In general, the phase shifters are required to have a higher power capacity, which can be increased by enhancing  $\Delta H$  or reducing  $4\pi M_s$ . However, the insertion loss of phase shifters will be increased when the power capacity is improved. To solve this problem, ferrite material with high saturation magnetization ( $4\pi M_s = 1950$  G) and low ferromagnetic resonance linewidth ( $\Delta H = 10$  Oe) is applied.

Computer simulation technology (CST) Microwave Studio is a commercially electromagnetic simulation software, whose numerical analysis is based on the finite integration technique (FIT) and full wave theory. By using this software, we can easily obtain the s-parameters and phase shift value of the

phase shifter. The boundary conditions are set as perfect electric conductor (PEC) along y and z axes, and open along x axis. The geometrical parameters were adjusted carefully by running numerous parameters sweeps and finally the optimal parameters for proposed configuration were obtained, as shown in Table 1. The optimized phase shifter has three adjacent operating bands with a large phase shift value.

**Table 1.** Parameters of the proposed phase shifter.

Parameter	Value (mm)	Parameter	Value (mm)
$a$	24.0	$b$	7.0
$l$	0.75	$r$	0.75
$n$	4.4	$z$	1.0
$t$	0.035	$h$	1.5

The changes of s-parameters and phase shift value with the applied magnetic field  $m$  are shown in Fig. 2. According to Fig. 2a, as  $m$  increases from 200 Oe to 500 Oe, the resonance frequency of the phase shifter moves to a higher frequency. As illustrated in Fig. 2b, the phase shift value of the phase shifter at the same frequency is affected by the applied magnetic field, indicating that the designed phase shifter has magnetically tunable characteristic. In addition, it can be observed from Fig. 2 that although the phase shifter has a desired phase shift about  $180^\circ$  in the range of 7.0-9.5 GHz, the frequency band with reflection coefficient less than -20 dB is very narrow.

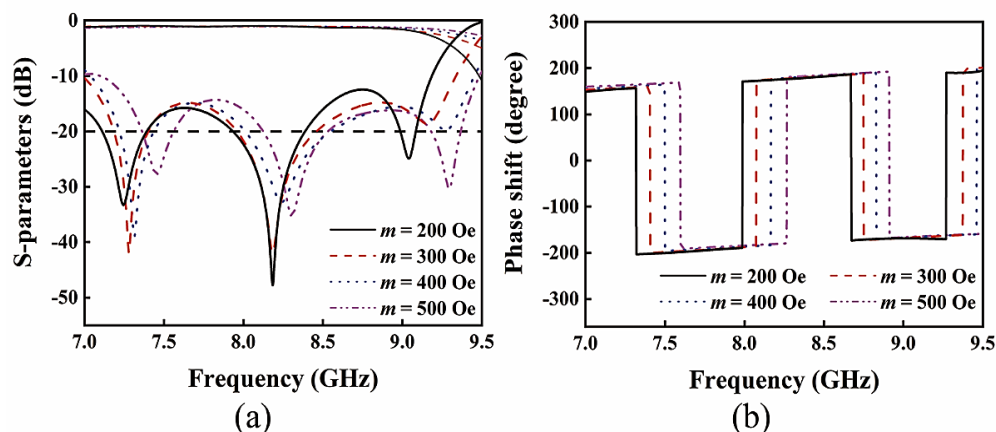


**Fig. 2** (a) Simulated s-parameters of the original phase shifter with a series of  $m$ . (b) Simulated phase shift of the original phase shifter with a series of  $m$ .

### 3. Metamaterial phase shifter

For realizing miniaturization or wideband, CRLH structure has been used in the design of phase shifters. In the range of the operating band, ferrite block can be equivalent to negative inductance, and the air-gap is utilized to act as negative capacitance. The top and bottom ferrite blocks in Fig. 1 are divided into three equal parts respectively, which are arranged periodically with the air-gap to form the metamaterial phase shifter. The geometry of the proposed metamaterial phase shifter is shown in Fig. 3.

To obtain the optimal parameters of the metamaterial phase shifter, the applied magnetic field is set to 500 Oe while the other parameters are consistent with Table 1. The impact of the width of the air-gap  $s$  on the proposed phase shifter is simulated as shown in Fig. 4. From Fig. 4a, the reflection coefficient changes significantly as  $s$  increases from 0.4 mm to 0.7 mm. When  $s = 0.5$  mm, the bandwidth with reflection coefficient less than -20 dB reaches the maximum. When the width of ferrite block and air-gap are respectively set to 8 mm and 0.5 mm, both the insertion loss and reflection coefficient meet the design requirements. Accordingly, the optimal parameters of the metamaterial phase shifter are obtained. In this condition,  $s$  only has little influence on the phase shift value of the metamaterial phase shifter as depicted in Fig. 4b.

Then, the s-parameters and phase shift value of the metamaterial phase shifter with different applied magnetic fields are simulated as shown in Fig. 5. It can be seen that

when  $m$  increases from 200 Oe to 500 Oe, the metamaterial phase shifter keeps wideband characteristic, which proves the reliability of the metamaterial phase shifter design. In addition, the simulated results of the original phase shifter and metamaterial phase shifter under different applied magnetic fields are compared. Similar to the original phase shifter, it can be found from Fig. 5a that the resonance frequency of the metamaterial phase shifter moves to a higher frequency with the increase of the applied magnetic field. According to Fig. 5b, the metamaterial phase shifter also exhibits magnetically tunable characteristic due to the metamaterial structure. In addition, it is discovered that Figs. 2b and 5b have a phase difference of  $360^\circ$  at the same frequency. From these simulated results, it can be inferred that the metamaterial introduces additional phase into the phase shifter, resulting in a great phase tunable range.

### 4. Results and discussion

In order to further demonstrate the performance of the metamaterial phase shifter, it is compared with the original phase shifter in s-parameters and voltage standing wave ratio (VSWR) with different applied magnetic fields. Fig. 6 describes the s-parameters of these phase shifters at different applied magnetic fields. From Fig. 6a, the original phase shifter has three resonant peaks while the metamaterial phase shifter has four resonant peaks in the range of 7.0-9.5 GHz. The additional resonant peak combines the three nearby bands

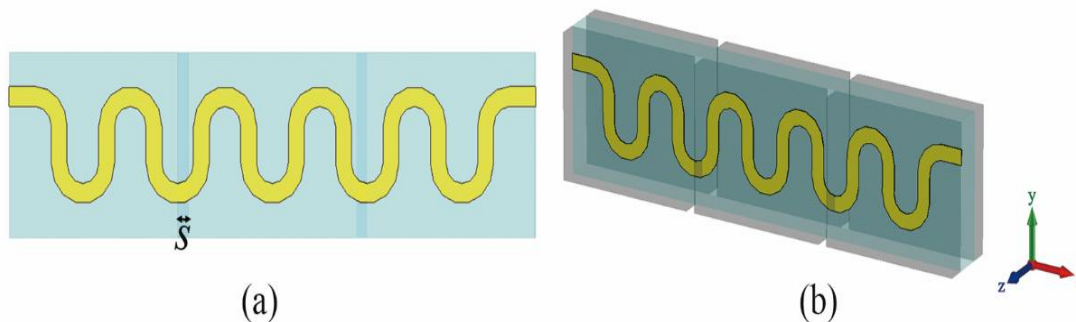


Fig. 3 Structure of the metamaterial phase shifter (a) top view and (b) perspective view.

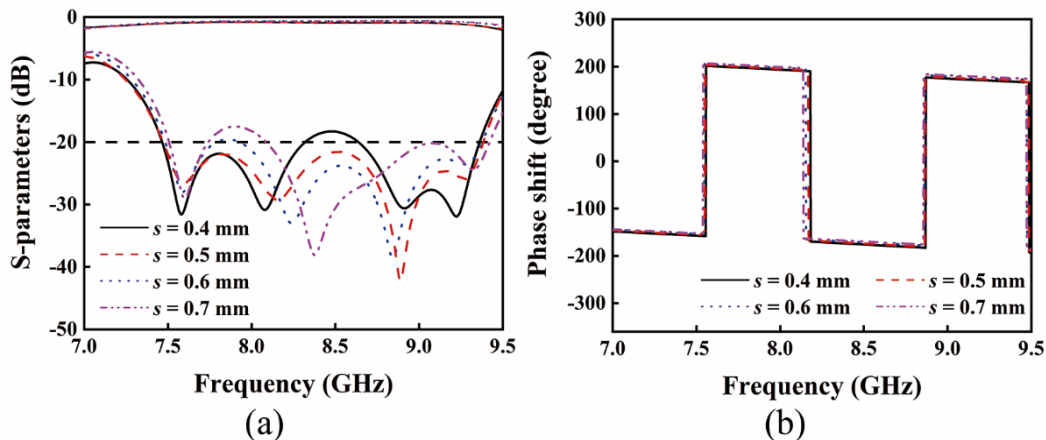
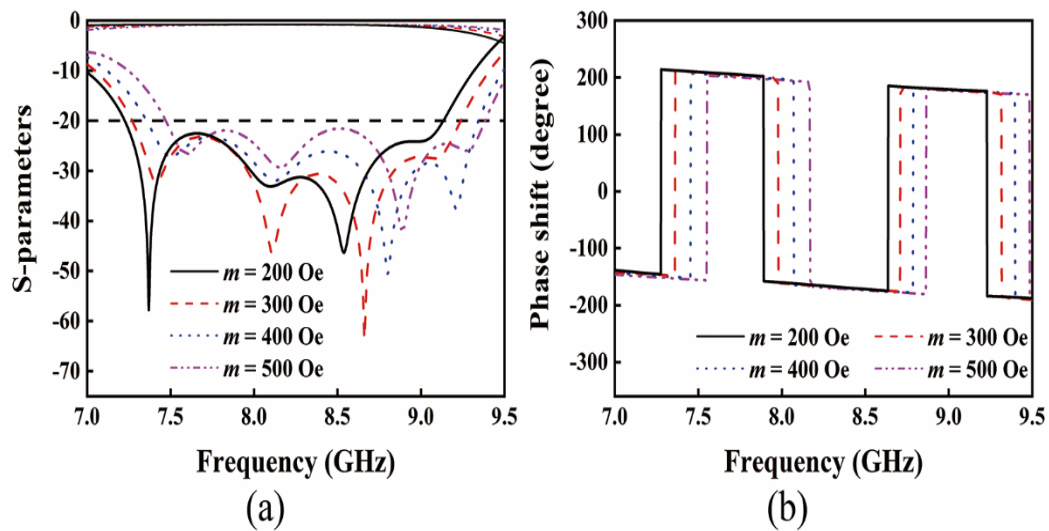


Fig. 4 (a) Simulated s-parameters of the metamaterial phase shifter with a series of  $s$ . (b) Simulated phase shift of the metamaterial phase shifter with a series of  $s$ .



**Fig. 5** (a) Simulated s-parameters of the metamaterial phase shifter with a series of  $m$ . (b) Simulated phase shift of the metamaterial phase shifter with a series of  $m$ .

into a single broadband, and thus the metamaterial phase shifter achieves a wider operating bandwidth. Moreover, the operating band of the metamaterial phase shifter moves to a higher frequency with the increase of applied magnetic field, which is consistent with the variation trend in Figs. 2 and 5. In general, the metamaterial phase shifter has wide bandwidth characteristic under different applied magnetic fields, which proves the reliability of the design.

Voltage standing wave ratio is a vital indicator used to measure whether the components are well matched. If the VSWR is equal to 1, it means that all the electromagnetic waves are radiated, which is the best case. In order to avoid the influence on other components, the VSWR of the devices should be as small as possible. Fig. 7 depicts the VSWR of these phase shifters with different applied magnetic fields. It can be found that the VSWR of the metamaterial phase shifter

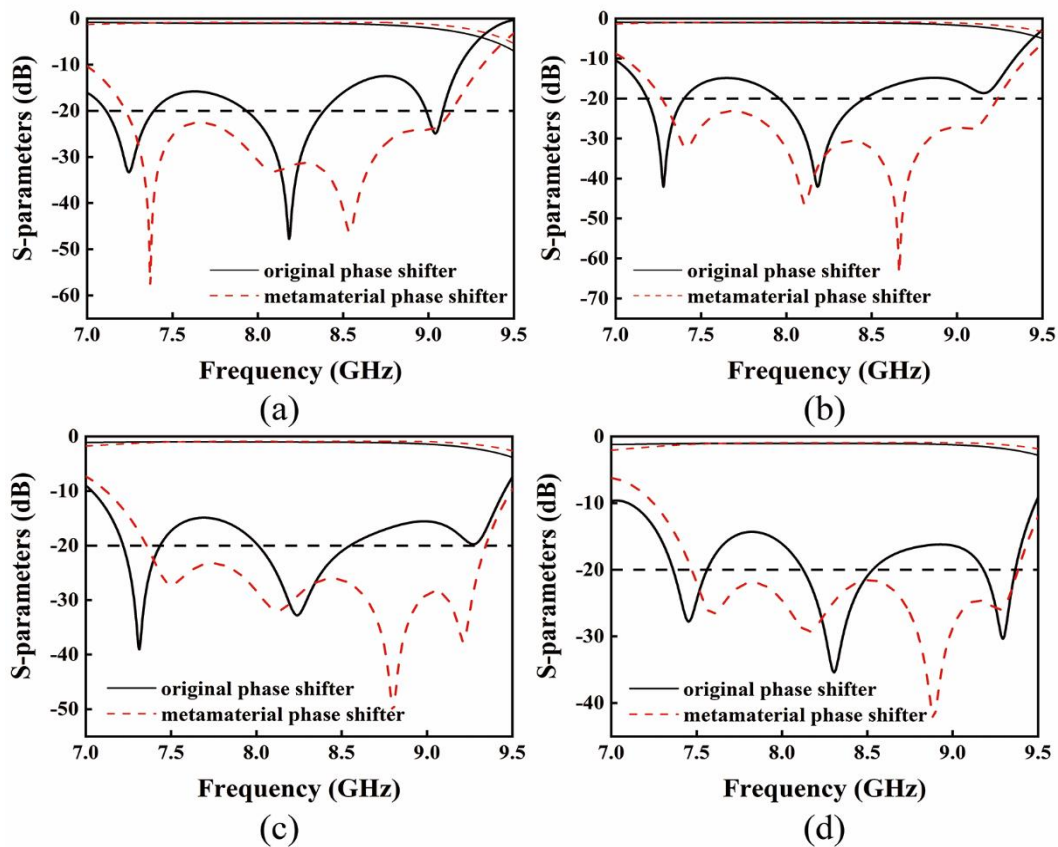


**Fig. 6** S-parameters of these phase shifters at different applied magnetic fields (a)  $m = 200$  Oe, (b)  $m = 300$  Oe, (c)  $m = 400$  Oe and (d)  $m = 500$  Oe.

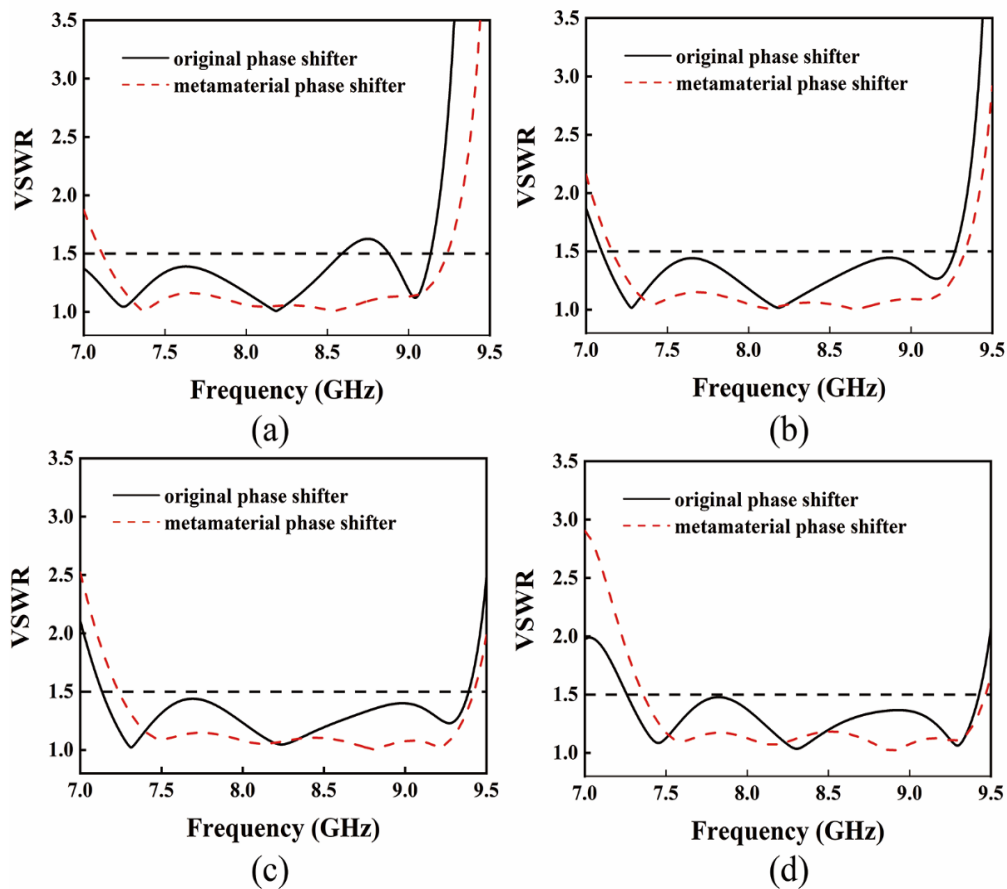


**Fig. 7** VSWR of these phase shifters at different applied magnetic fields (a)  $m = 200$  Oe, (b)  $m = 300$  Oe, (c)  $m = 400$  Oe and (d)  $m = 500$  Oe.

is basically stable at 1 in the operating band, which shows the impedance matching of the metamaterial phase shifter is excellent. To sum up, the proposed metamaterial phase shifter with relative operation bandwidth greater than 20% has a few advantageous features, such as inclusive of simple structure, large phase shift value, good impedance matching and easy adjustment in phase shift.

To illustrate the working principle of the metamaterial phase shifter, the distribution of electromagnetic fields in the microstrip line is simulated. Fig. 8 shows the electric and

magnetic distributions of the material phase shifter at 8.9 GHz. From Fig. 8, it can be observed that the intensity of the electromagnetic fields is the largest at the edge of the meander line microstrip. Moreover, the distribution of the electromagnetic fields is periodic. As we known, the permeability of ferrite materials varies with the magnetic field. Hence, it can be deduced that the phase shift value will also has periodicity, which is in concordance with the simulated results. This model can realize the function of phase shift well.

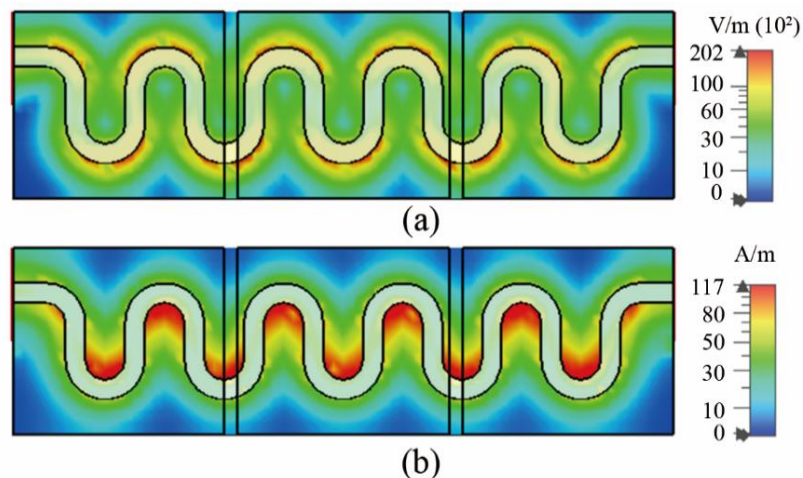


**Fig. 8** Distribution of electromagnetic fields in the microstrip line (a) electric field and (b) magnetic field.

## 5. Conclusions

In this paper, a tunable metamaterial ferrite phase shifter with relative bandwidth greater than 20% is developed. According to the s-parameters simulated results, the metamaterial phase shifter can stimulate a new resonant peak that coupled with the inherent resonant peaks, which can help to get the wideband property. Moreover, the periodic change of phase shift value with frequency can be explained by the distribution of electromagnetic fields in the microstrip line. Our work realizes both adjustability and wideband in a phase shifter, which gives an effective approach for tunable and wideband design of the ferrite-based phase shifters.

## Acknowledgements

This work was supported by the National Natural Science Foundation of China (Grant Nos. 61774020, 51972033, 51788104, and 61976025), Beijing Youth Top-Notch Talent Support Program, and Key area research plan of Guangdong (Grant No. 2019B010937001).

## Conflict of interest

There are no conflicts to declare.

## Supporting information

Not applicable.

## References

- [1] P. K. Deb, T. Moyra and B. K. Bhattacharyya, *Electromagnetics*, 2020, **40**, 207-216, doi: 10.1080/02726343.2020.1726072.
- [2] G. J. Deng, W. H. Huang, J. W. Li, H. Shao, L. T. Guo and S. Y. Xie, *Rev. Sci. Instrum.*, 2019, **90**, 114705, doi: 10.1063/1.5125843.
- [3] M. M. Teymoori, M. Dousti and S. Afrang, *Int. J. Circ. Theor. App.*, 2020, **48**, 2111-2129, doi: 10.1002/cta.2871.
- [4] Z. Liang, Q. Liu and T. Long, *IEEE T. Instrum. Meas.*, 2020, **69**, 7365-7376, doi: 10.1109/tim.2020.2984417.
- [5] W. Zhang, C. Zhang, Z. Zhao, F. Liu and T. Chen, *Circ. Syst. Signal Pr.*, 2020, **39**, 420-438, doi: 10.1007/s00034-019-01192-0.
- [6] X. Chen, Y. Wu, Y. Yang and W. Wang, *IEEE Access*, 2020, **8**, 82286-82293, doi: 10.1109/access.2020.2991163.
- [7] J. Zhang, T. Li, R. Kokkonen, C. Yan, W. Liu, M. Partanen, K. Y. Tan, M. He, L. Ji, L. Gronberg and M. Mottonen, *AIP Adv.*, 2020, **10**, 065128, doi: 10.1063/5.0006499.
- [8] G. Chaudhary and Y. Jeong, *IEEE Microw. Wirel. Co.*, 2019, **29**, 468-470, doi: 10.1109/lmwc.2019.2920270.
- [9] Y.-P. Lyu, L. Zhu and C.-H. Cheng, *IEEE T. Microw. Theory*, 2020, **68**, 5221-5234, doi: 10.1109/tmtt.2020.3027842.
- [10] Y.-P. Lyu, L. Zhu, Q.-S. Wu and C.-H. Cheng, *IEEE T. Microw. Theory*, 2016, **64**, 4211-4221, doi: 10.1109/tmtt.2016.2608889.
- [11] H. Al-Saedi, W. M. Abdel-Wahab, S. Gigoyan, A. Taeb and S. Safavi-Naeini, *Int. J. Microw. Wirel. T.*, 2018, **10**, 77-86, doi: 10.1017/s1759078717001118.
- [12] F. A. Ghaffar and A. Shamim, *IEEE T. Magn.*, 2015, **51**, 4003108, doi: 10.1109/tmag.2015.2404303.
- [13] M. A. Abdelaal, S. I. Shams and A. A. Kishk, *IEEE Access*, 2019, **7**, 23766-23778, doi: 10.1109/access.2019.2899567.
- [14] B. A. Belyaev, K. V. Lemberg, A. M. Serzhantov, A. A. Leksikov, Y. F. Bal'va and A. A. Leksikov, *IEEE T. Magn.*, 2015, **51**, 4003205, doi: 10.1109/tmag.2014.2368513.
- [15] G.-M. Yang, J. Lou, O. Obi and N. X. Sun, *IEEE Microw. Wirel. Co.*, 2011, **21**, 240-242, doi: 10.1109/lmwc.2011.2123085.
- [16] M. Yasir, S. Bistarelli, A. Cataldo, M. Bozzi, L. Perregrini and S. Bellucci, *IEEE Microw. Wirel. Co.*, 2019, **29**, 47-49, doi: 10.1109/lmwc.2018.2882309.
- [17] Z. R. Omam, W. M. Abdel-Wahab, A. Pourziad, S. Nikmehr, A. Palizban, S. Gigoyan and S. Safavi-Naeini, *IEEE Microw. Wirel. Co.*, 2020, **30**, 485-488, doi: 10.1109/lmwc.2020.2980264.
- [18] W. Zhang, Z. Shen, K. Xu and J. Shi, *IEEE Microw. Wirel. Co.*, 2019, **29**, 767-770, doi: 10.1109/lmwc.2019.2949681.
- [19] L. Wang, D. Xia, Q. Fu, X. Ding and Y. Wang, *Front. Phys.-Lausanne*, 2020, **8**, 303, doi: 10.3389/fphy.2020.00303.
- [20] X. Fu, L. Shi and T. Cui, *J. Mater. Eng.*, 2020, **48**, 12-22, doi: 10.11868/j.issn.1001-4381.2019.000849.
- [21] H. Du, Z. Zhang, R. Tian, W. Zhang, J. Zhang, X. Liu, K. Sun and R. Fan, *J. Mater. Eng.*, 2020, **48**, 23-33, doi: 10.11868/j.issn.1001-4381.2019.001015.
- [22] S. Sheng, H. Chen, J. Wen and H. Liu, *Radioengineering*, 2019, **28**, 585-590, doi: 10.13164/re.2019.0585.
- [23] Z. He, S. An, J. Liu and C. Jin, *IEEE Access*, 2020, **8**, 140438-140444, doi: 10.1109/access.2020.3012596.
- [24] M. A. B. Abbasi, M. A. Antoniadou and S. Nikolaou, *IEEE T. Antenn. Propag.*, 2018, **66**, 1025-1030, doi: 10.1109/tap.2017.2777520.
- [25] D. Gonzalez-Andrade, J. M. Luque-Gonzalez, J. G. Wanguemert-Perez, A. Ortega-Monux, P. Cheben, I. Molina-Fernandez and A. V. Velasco, *Photonics Res.*, 2020, **8**, 359-367, doi: 10.1364/prj.373223.
- [26] M. Shafae, S. M. J. Razavi and E. Hamidi, *Microw. Opt. Techn. Lett.*, 2019, **61**, 1692-1696, doi: 10.1002/mop.31800.
- [27] J. Ghalibafan, N. Komjani and B. Rejaei, *Electromagnetics*, 2013, **33**, 234-248, doi: 10.1080/02726343.2013.769407.

## Authors information

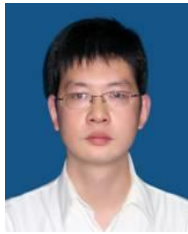


**Huiming Yao** received the B.Sc. degree in physics from Beijing University of Posts and Telecommunications in 2021. She is now pursuing her Ph.D. degree in Beijing University of Posts and Telecommunications. Her research interests include metamaterials

and antenna design.



**Shihong Wang** received her Ph.D. from Beijing Normal University. She worked as a visiting scholar at the University of California, Los Angeles from January to August in 2007. She is now a professor in Beijing University of Posts and Telecommunications. Her research group focuses on nonlinear dynamics and complex networks.



**Ming Lei** received his Ph.D. from Chinese academy of science in 2007. He worked as a postdoctoral fellow at the Hong Kong University of Science and Technology and Chinese University of Hong Kong from 2007 to 2008 and from 2009 to 2010, respectively. He is now a professor in Beijing University of Posts and Telecommunications. His research group focuses on synthesis of low-dimensional semiconductor and related photoelectric properties.



**Ke Bi** received his Ph.D. from Nanjing University of Aeronautics and Astronautics in 2012. From 2012 to 2014, he worked as an assistant researcher in Tsinghua University. He is now a professor in Beijing University of Posts and Telecommunications. His research group focuses on information functional materials and devices, electromagnetic metamaterials and devices.

**Publisher's Note:** Engineered Science Publisher remains neutral with regard to jurisdictional claims in published maps and institutional affiliations.